

# Variational Analysis of Dielectrically Loaded Multidepth Corrugated Waveguides

MARKKU I. OKSANEN

**Abstract** — The propagation behavior in a multidepth corrugated waveguide is analyzed. The analysis is based on the theory of nonstandard eigenvalues and variational methods. This method is tested for an empty dual-depth corrugated guide, the results of which have been previously calculated in the literature by using surface impedance and space harmonic methods. These methods are summarized here. Also, space harmonic formulas are rederived in the form where the fundamental surface admittance component is separated from the higher order terms. It is seen that, with elementary trial functions, very accurate dispersion relations can be obtained by the variational method. Encouraged by this, the method is then extended for a tridepth guide operating in three different frequency bands, and for dielectrically loaded dual- and tridepth guides. The latter components may hold considerable promise because of their simpler fabrication technique.

## I. INTRODUCTION

SINGLE- AND dual-depth corrugated horns or waveguides have found applications in cases where pattern symmetry related to low cross-polarization is required. In a single-depth horn, these characteristics can be realized at a certain frequency band around the balanced frequency of the horn. At that frequency the depth of the corrugation slot is approximately a quarter of the wavelength. When the corrugation consists of two different slot depths, i.e. a dual-depth horn, these requirements can be met in two separate frequency bands. The ratio of the depths of the two slots, and hence the ratio of the operating bands, can vary between 1:1.3 and 1:2.0 [1].

Since the invention of the dual-depth corrugated guide, various theoretical methods have been introduced to analyze wave propagation and radiation characteristics of such a horn. The first one [2] is based on an average wall admittance, an assumption which can be justified as an approximation if the depths of the slots do not differ much from each other. In this method, relation between the fields in the adjacent slots are not taken into account. This is valid also for the surface impedance method, which assumes infinitely thin corrugations [3]. Including field coupling between the slots and realistic corrugation dimensions requires a space harmonic analysis [1], [4]–[7]. In this method the fields in the central propagation region are

represented by a summation of a fundamental harmonic and pairs of space harmonics. In the first variation of the method, the slot pitches were assumed to be sufficiently small compared with the wavelength, so that higher order  $TE_{nm}$  and  $TM_{nm}$  evanescent waves in the slots could be neglected [4], [5]. In more exact analyses, these slot modes are included [1], [6], [7]. The optimum combination for the numerical calculations is reached when the number of slot mode pairs equals that of the space harmonic pairs. Usually three pairs are sufficient in order to have an acceptable accuracy.

If the space harmonics are neglected, one obtains a modified surface impedance model with certain coefficients which include the information of the corrugation geometry. This model predicts the propagation performance of a guide very accurately, particularly for the basic  $HE_{11}$  mode, as is shown graphically in [7]. The effect of space harmonics manifests itself mainly in the cross-polar radiation behavior of the horn: the peak cross-polar level rises and the frequency at which the minimum cross-polar level occurs is lowered when harmonics are taken into account [1], [6], [7].

A different approach to handle corrugated waveguides relies on the theory of nonstandard eigenvalues and variational principles introduced in [8]. The eigenvalue parameter is the boundary susceptance of the corrugated surface. The resulting simple functional was shown to give accurate dispersion relations for air-filled single-depth corrugated guides. The method was then applied to a dielectrically loaded waveguide, which because of the simple fabrication technique can be used instead of the air-filled counterpart. It was shown that the variational method can be successfully applied also for the corrugated guide with the dielectric insert.

In this report, this method is extended to dual-depth and tridepth corrugated waveguides. Both geometries are analyzed with and without a dielectric load. The waveguide is assumed to be straight. Section II discusses geometry, stationary functional, trial fields, eigenvalue equations, and surface impedance formulas of the multidepth corrugated guide. In Section III dispersion curves obtained by the variational method are depicted and results are compared with those calculated by other methods. Section IV applies the theory to a dielectrically loaded waveguide, and Section V contains the conclusion of the present work.

Manuscript received February 17, 1988; revised July 5, 1988. This work was supported by grants from the Academy of Finland, the Emil Aaltonen Foundation, and the Jenny and Antti Wihuri Foundation.

The author is with the Faculty of Electrical Engineering, Helsinki University of Technology, Otakaari 5A, SF-02150 Espoo, Finland.

IEEE Log Number 8824267.

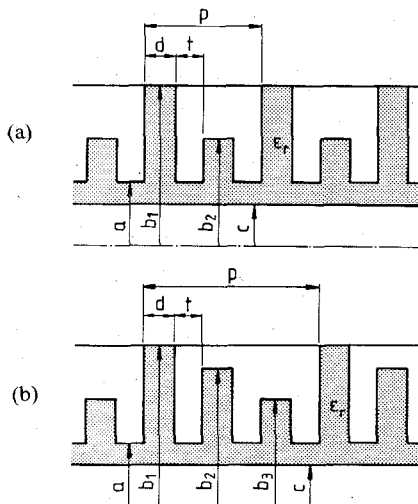


Fig. 1. Dielectrically loaded (a) dual-depth and (b) tridepth corrugated wave-guides.

## II. THE MULTIDEPTH CORRUGATED WAVEGUIDES

Consider a multidepth corrugated waveguide which is uniform in the axial  $z$  direction and possibly filled with a dielectric medium  $\epsilon(\rho)$  which can be homogeneous or nonhomogeneous. The surface of the waveguide consists of adjacent slots whose depth varies in series. The cross section of the guide with two or three different slot depths in a single corrugation period is shown in Fig. 1. The inner radius of the guide is denoted by  $c$ ,  $a$  is the radius measured to the ridge, with width  $t$ ,  $d$  is the width of the slot, and  $b_1$  and  $b_2$  (or  $b_3$ ) are the radii of the deeper and shallowest (or shallowest) slots, respectively.

### A. A Stationary Functional for the Boundary Susceptance

If the field solutions are written as  $\bar{E}(\rho)e^{-j\beta z}$  and  $\bar{H}(\rho)e^{-j\beta z}$  and transversal fields are eliminated, the following stationary functional for the boundary admittance  $Y_s$ , or for the boundary susceptance  $B_s$ , of the transversely corrugated waveguide can be derived [8]:

$$Y_s = \frac{j\omega}{\phi e^2 d C} \int \left[ k_c^{-2} \left( \epsilon(\nabla e)^2 + 2 \frac{\beta}{\omega} \bar{u} \cdot \nabla e \times \nabla h + \mu(\nabla h)^2 \right) - \epsilon e^2 - \mu h^2 \right] dS = jB_s. \quad (1)$$

Here,  $k_c^2(\rho) = \omega^2 \mu(\rho) \epsilon(\rho) - \beta^2$ , with  $\omega$  the angular frequency and  $\beta$  the propagation factor. The surface integral is taken over the cross section of the guide to the corrugation boundary, and the contour integral goes along that boundary. The functional can handle circular cross sections as well as cross sections of arbitrary shape.

This is the basic equation in our analysis. To apply it, we have to insert suitable trial functions for the fields  $e$  and  $h$ , from which the expression for the surface admittance can be calculated. In a corrugated waveguide the latter can be approximated by certain formulas. This and trial field choices are discussed in the following subsections.

### B. Trial Fields

Consider an empty air-filled multidepth corrugated waveguide where the dielectric insert has  $\epsilon_r = 1.0$  in Fig. 1. In the following we assume that all slots and ridges have the same widths  $d$  and  $t$ , respectively. This assumption can be justified by an easier fabrication technique.

In a space-harmonic formulation, the longitudinal electric and magnetic fields in the circular corrugated waveguide for  $\rho \leq a$  are [1], [4]–[7]

$$e = \sum_{N=-K}^K C_N Z_{nN}(k_{cN}\rho) \cos n\phi e^{-j\beta_N z} \quad (2)$$

$$h = \sum_{N=-K}^K D_N Z_{nN}(k_{cN}\rho) \sin n\phi e^{-j\beta_N z} \quad (3)$$

where  $C_N$  and  $D_N$  are arbitrary coefficients,  $Z_{nN}(k_{cN}\rho) = J_n(k_{cN}\rho)/J_n(k_{cN}a)$ , and  $(k_{cN}\rho)^2 = (k\rho)^2 - (\beta_N\rho)^2$ .  $J_n$  stands for a Bessel function of the first kind of order  $n$ . In theory  $K = \infty$ , but  $K = 1$  has been found to be sufficient for the field calculations [1], [6]. Accurate fields can be calculated even for  $K = 3$  [1], [6]. The propagation factor  $\beta_N = \beta + 2\pi N/p$  consists of the fundamental harmonic term  $\beta$  and of the periodicity factor  $2\pi N/p$ , with  $p$  the period of the corrugation. In a dual-depth waveguide  $p = 2d + 2t$ , and in a tridepth guide  $p = 3d + 3t$  (see Fig. 1). This parameter relates the fields in one cell to those in the next. The fields in the remaining part of the guide, in the slot region, are now not needed because the boundary is taken into account by a proper admittance. Next we limit the analysis to the lowest order  $HE_{1m}$  and  $EH_{1m}$  modes whence  $n = 1$  in (2) and (3). Since  $J_1(x)$  is an odd polynomial, physical intuition shows that trial fields in the functional must be of the form

$$e(\rho, \phi) = ((1-\alpha)(\rho/a) + \alpha(\rho/a)^3) \cos \phi = g(\rho) \cos \phi \quad (4)$$

$$h(\rho, \phi) = Ag(\rho) \sin \phi. \quad (5)$$

The parameters  $\alpha$  and  $A$  must be determined through the functional. Inserting (4) and (5) into (1) and requiring  $\partial Y_s / \partial A = 0$  and  $\partial Y_s / \partial \alpha = 0$  gives

$$A_{\text{opt}} = \frac{\beta}{\omega \mu} \frac{1}{\frac{(ak_c)^2(6-4\alpha_{\text{opt}}+\alpha_{\text{opt}}^2)}{24} - 1 - \frac{2\alpha_{\text{opt}}^2}{3}} \quad (6)$$

$$\alpha_{\text{opt}} = \frac{2(k_c a)^2}{(k_c a)^2 - 16}. \quad (7)$$

The use of these trial functions is very convenient because both parameters can be obtained analytically, and numerical optimization routines can be totally avoided. Since the surface admittance was chosen for the eigenvalue parameter, optimized trial fields do not depend on the particular surface corrugation, and the fields (4) and (5) together with their optimized parameters can be applied in connection with any kind of corrugation geometry.

There is one additional advantage in using the above trial fields. If we demand that  $\alpha = 0$ , insert the fields in the functional, and carry out the calculations, the dispersion relation is seen to be solved analytically [8]:

$$\beta a = \sqrt{\frac{((ka)^2 - 4)((ka)^2 + 4ka\eta B_s - 4)}{ka(ka + 4\eta B_s)}}. \quad (8)$$

Again, the application of this formula is not limited to a particular boundary susceptance.

### C. Space Harmonic and Surface Impedance Formulas

The eigenvalue equation of the air-filled corrugated waveguide can be derived by matching the fields in the central region to the fields in the slots at the common boundary  $\rho = a$ . If the widths of the slots are much smaller than the wavelength, i.e.,  $d \ll \lambda$ , only the lowest order  $\text{TM}_{10}$  mode is required in the slot. This assumption simplifies the eigenvalue equation into the following form [1], [3]–[5]:

$$k_{c0}aZ'_{n0}(k_{c0}a) - \frac{n^2(\beta a)^2}{(ka)^2(k_{c0}a)Z'_{n0}(k_{c0}a)} = \frac{(k_{c0}a)^2}{ka} Y_d \quad (9)$$

with  $k_{c0}^2 = k^2 - \beta^2$ . The prime denotes the first derivative with respect to the argument.  $Y_d$  stands for the equivalent admittance of the corrugated surface. It is related to the surface admittance  $Y_s$  and to the susceptance  $B_s$  by the relations  $Y_s = jB_s = jY_d/\eta$  with  $\eta = \sqrt{\mu/\epsilon}$ . For the exact equation, all  $\text{TE}_{nm}$  and  $\text{TM}_{nm}$  standing waves in the slots are required. The eigenvalue equation would then be of a determinant type and must be solved iteratively [1], [6], [7]. When considering the most important  $\text{HE}_{11}$  and  $\text{EH}_{12}$  modes, the influence of these higher order slot modes is concentrated in the regions near the high-frequency cutoff point in the dispersion diagram for the  $\text{HE}_{11}$  mode and in the region of the short-circuit condition for the  $\text{EH}_{12}$  mode [7]. The high-frequency condition appears when the parameter  $\beta a$  tends to infinity or, more exactly,  $\beta p$  equals  $\pi$ . This happens in the unimportant slow-wave part of the dispersion diagram, far from the balanced frequency points. At the short-circuit condition the equivalent impedance is zero. In addition, the slot modes also have an effect on the cross-polarization performance of the guide, a subject which is beyond the scope of this study. Thus this simplified space-harmonic analysis is well motivated when only the dispersion characteristics of the basic  $\text{HE}_{11}$  mode are of concern.

The formula for the equivalent admittance is given in [5]. Here we write it in a form where the fundamental admittance component  $y_0$  is separated from the terms  $y_{h1}$  and  $y_{h2}$  related to the higher order harmonics:

$$Y_d = y_0 + y_{h1} + y_{h2}, \quad (10)$$

where

$$y_0 = \frac{p}{2d} \frac{1}{S_0^2} \left[ \frac{2y_1 y_2}{y_1 + y_2} \right] \quad (11)$$

$$y_{h1} = -\frac{1}{2S_0^2} W_{s1} \frac{(y_1 - y_2)^2}{(y_1 + y_2)} \frac{1}{\left[ y_1 + y_2 - \frac{2d}{p} W_{s1} \right]} \quad (12)$$

$$y_{h2} = -\frac{1}{2S_0^2} W_{s2}, \quad (13)$$

and

$$W_{s1} = \sum_{N=-K}^K S_N^2 \frac{ka}{(k_{cN}a)^2} F_N [1 - (-1)^N] \quad (14)$$

$$W_{s2} = \sum_{N=-K}^K S_N^2 \frac{ka}{(k_{cN}a)^2} F_N [1 + (-1)^N] \quad (N \neq 0) \quad (15)$$

$$F_N = k_{cN}aZ'_{nN}(k_{cN}a) - \frac{n^2(\beta_N a)^2}{(ka)^2 k_{cN}aZ'_{nN}(k_{cN}a)} \quad (16)$$

$$S_N = \sin(\beta_N d/2)/(\beta_N d/2) \quad (17)$$

$$y_i = \frac{J'_n(ka)Y_n(kb_i) - Y'_n(ka)J_n(kb_i)}{J_n(ka)Y_n(kb_i) - Y_n(ka)J_n(kb_i)}, \quad i = 1, 2. \quad (18)$$

Here  $Y_n$  is a Bessel function of the second kind of order  $n$ . In realistic corrugated waveguides the period of the corrugation is normally much smaller than the wavelength or the radius of the guide, i.e.,  $p \ll \lambda$  and  $a$ . Thus, if we assume as in [4] that  $\beta_N \approx 2N\pi/p$ ,  $k_N \approx j|\beta_N|$ , and  $Z'_{nN}(k_N a) \approx -j$ , the series terms can be simplified:

$$W_{s1} = -\frac{2p}{\lambda} \sum_{N=1}^K \frac{\sin^2(N\pi d/p)}{(N\pi d/p)^2} \left( 1 - \frac{n^2}{(ka)^2} \right) \cdot (1 - (-1)^N) \frac{1}{N} \quad (19)$$

$$W_{s2} = -\frac{2p}{\lambda} \sum_{N=1}^K \frac{\sin^2(2N\pi d/p)}{(2N\pi d/p)^2} \left( 1 - \frac{n^2}{(ka)^2} \right) \frac{1}{N}. \quad (20)$$

These expressions are easier to compute than those in (14) and (15).

Terms  $y_1$  and  $y_2$  can be interpreted as equivalent admittances of the two slots. In fact,  $y_1$ , or  $y_2$ , is the exact TEM admittance formula, which is a good approximation for the single-depth corrugated surface if the period of the corrugation is small enough.

The surface impedance formulation applies to (11) only. In its traditional form [3]  $t/d = 0$  is assumed, indicating infinitely thin corrugations. Also  $\sin(\beta d/2) = \beta d/2$ , whence the term in front of the parenthesis in (11) approximately equals to 1. The coefficient 2 remains so the equivalent admittance of the corrugation is seen to be twice the series admittance of the slots. The equivalent admittance  $y_i$  of a single slot, whose depth is  $b_i - a$ , can be

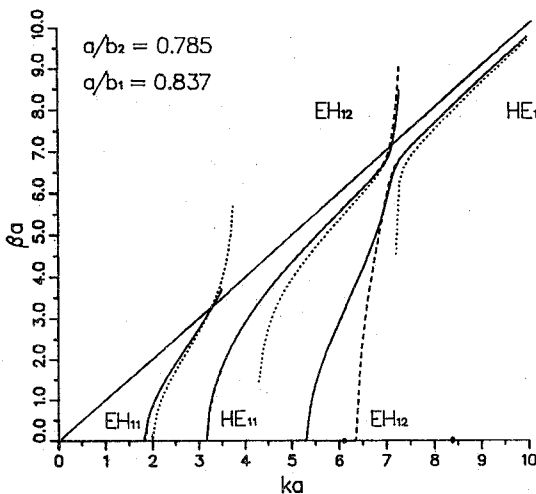


Fig. 2. Dispersion curve for an empty dual-depth corrugated waveguide. The parameters are  $a/b_1 = 0.837$ ,  $a/b_2 = 0.785$ ,  $t/d = 0.15$ , and  $d/a = 0.10$ . The balanced frequencies are marked by the spots. The solid line refers to the surface impedance method (eqs. (9)–(11)), the dashed line refers to the variational method with the cubic test function and the optimized parameters, (eqs. (1), (4)–(7)). The dotted line refers to the analytical equation (8).

approximated by the following formula [8]:

$$y_i = \eta B_s = -\cot(k(b_i - a)) + \frac{1}{2ka} \quad (21)$$

which is valid for large  $ka$  values. In the limit  $ka \gg 1$  the latter term in the formula can be neglected. If  $k(b_i - a)$  is small enough, we obtain another approximation for the admittance. In this paper (21) is applied in all variational calculations.

In the above analysis we have considered the dual-depth corrugation. If the corrugation consists of more adjacent slots, the equivalent admittance can be formed by the series connection of the single-slot admittances.

### III. NUMERICAL RESULTS

To verify the method for multidepth corrugations we have analyzed dual-depth and tridepth geometries. The analysis includes dispersion properties of such guides without handling co- and cross-polarization radiation patterns, which are well treated by the space-harmonic methods and by the Fourier transform technique. The accuracy of the present theory is studied by comparing the results with those obtained by using the space-harmonic and surface impedance formulas.

#### A. A Dual-Depth Corrugated Waveguide

Two different corrugation geometries were considered. In the first example the depths of the slots were  $a/b_1 = 0.837$  and  $a/b_2 = 0.785$ . This combination corresponds to the frequency band ratio 1:1.406 with the balanced frequencies at  $ka = 8.4123$  and at  $ka = 6.0901$ . In the second example these figures were  $a/b_1 = 0.837$  and  $a/b_2 = 0.71969$ , the frequency band ratio was 1:2, and the balanced frequency points were at  $ka = 8.4123$  and  $ka = 4.3979$ . The corrugation parameters were chosen as  $t/d =$

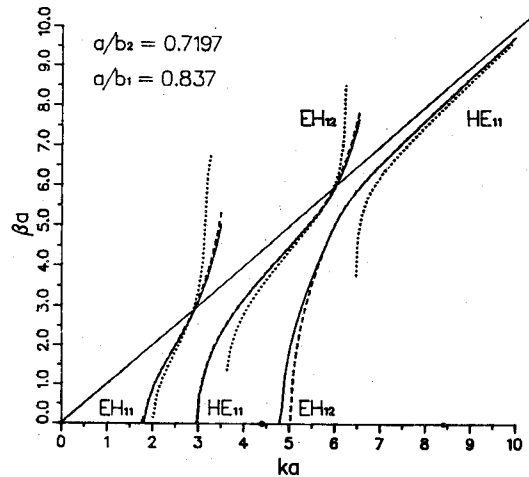


Fig. 3. Same as in Fig. 2 for  $a/b_1 = 0.837$  and  $a/b_2 = 0.71969$ .

0.15 and  $d/a = 0.10$ , which could be realistic values. For example if  $a = 40$  mm we had  $d = 4$  mm and  $t = 0.6$  mm. Dispersion curves can now be obtained by inserting fields (4) and (5) with (6) and (7) into (1). Figs. 2 and 3 show show the results for both guides. The solid curve refers to the surface impedance method (9) and (10) with (11)) and the dashed and dotted lines refer to the variational method with the cubic and the linear test functions, respectively. The mode designation is that given in [1]. The  $HE_{11}$  mode has two branches: the first from the low-frequency cutoff to the point  $\beta/k = 1$  and the second from the high-frequency part down to the  $EH_{12}$  mode cutoff. The balanced frequencies are marked in both figures. The functional equation with the cubic trial fields is seen to follow the surface impedance curve very closely, except near the  $EH_{12}$  low-frequency cutoff, where the former predicts a cutoff point too high. The analytical dispersion formula (8) is most accurate when the  $\beta/k = 1$  curve is approached.

To obtain concrete values of the accuracy we have calculated normalized propagation  $\beta a$  at different normalized frequency points  $ka$  in Table I. The geometry of the guide is that of the second example given above. The  $ka$  values are taken so that  $ka = 2.5$ –3 are from the  $EH_{11}$  mode,  $ka = 4.3979$ –6.2 are from the  $HE_{11}$ – $EH_{12}$  mode, and  $ka = 6.5$ –10 are from the  $EH_{12}$ – $HE_{11}$  mode.

From Table I we find that the variational method with the linear test function (column A) is most inaccurate with the error in the dispersion relation ranging from a few percent to tens of percent. On the other hand, it is the only method which gives an analytical eigenvalue equation and thus is very easy to apply. The variational functional with the cubic test function, column B, seems to work very well in the whole region, except at the values near the  $EH_{12}$  mode high- and low-frequency cutoffs. The accuracy would probably have been better if instead of (21) we had used (18) for the single slot admittance. However, (21) does not include special functions, which in some cases can be advantageous. Column C represents the traditional surface impedance method introduced in [3]. When these results are compared with those from the space-harmonic analysis

TABLE I  
VALUES OF THE NORMALIZED PROPAGATION PARAMETER  $\beta a$  FOR DIFFERENT VALUES OF THE NORMALIZED FREQUENCY  $ka$   
AND THE CORRESPONDING ERROR IN PERCENT

A		B		C		D		E		F	
$ka$	$\beta a$	%	$\beta a$	%	$\beta a$	%	$\beta a$	%	$\beta a$	%	$\beta a$
2.5	1.8375	-8.304	2.0149	.549	2.079	3.748	1.9997	-.210	2.005	.055	2.0039
3.0	3.3892	7.301	3.1883	.940	3.373	6.788	3.126	-1.032	3.1648	.196	3.1586
4.3979	3.5154	-6.351	3.7343	-.519	3.7246	-.778	3.7246	-.778	3.7590	.139	3.7538
5.5	5.0806	-4.995	5.1477	-3.741	5.1245	-4.174	5.1313	-4.047	5.670	.361	5.3477
6.2	7.099	-14.099	6.5205	-21.10	6.6531	19.495	6.4383	-22.09	7.9057	-4.338	8.2642
6.5	4.6673	-21.98	5.9026	-1.133	5.9291	-.888	5.8980	-1.408	5.9816	-.010	5.9822
8.4123	7.9389	-1.792	8.0662	-.218	8.0664	.215	8.0664	-.215	8.0808	-.037	8.0838
10.	9.6628	-2.452	9.7381	-1.692	9.7330	1.743	9.7376	-1.726	9.7970	-1.097	9.9057

The waveguide is a dual-depth corrugated guide with the parameter values  $a/b_1 = 0.837$ ,  $a/b_2 = 0.71969$ ,  $t/d = 0.15$ , and  $d/a = 0.10$ . The balanced frequencies are at  $ka = 4.3979$  and at  $ka = 8.4123$ . Columns A and B refer to the variational results with the linear test function (eq. (8)) and with the cubic test function, respectively. Columns C and D refer to the surface impedance method (eqs. (9)–(11)), where in column C the term in front of the parenthesis in (11) is marked as 1 [3], and in column D eq. (11) is directly applied. Columns E and F refer to the space-harmonic analysis (eqs. (9)–(20)). The results in column E are obtained from the approximations (19) and (20) with  $K = 17$ . Column F has been calculated by using (14) and (15) with  $K = 8$ .

with only the fundamental component included (column D), one finds that the former is in some parts of the dispersion curve even more accurate than the latter. The approximation made in column C can be adequately justified when the corrugation is dense enough, in which case these two columns should give results very much alike. The assumption of the dense corrugation is also made in column E. Again, if the slots and the ridges are very thin, the error should be very small. Column F has been calculated from the space-harmonic equations. These results differ from the exact space harmonic analysis, which includes the slot modes, only in the regions near the high-frequency cutoff and near the short-circuit condition of the  $EH_{12}$  mode [7]. Some estimates for the accuracy are given in [9] for the single-depth guide and for the  $HE_{11}$  mode. The difference between the high-frequency  $ka$  values of the surface impedance model and those of the exact space-harmonic model has been calculated to be over 12 percent for the single-depth guide with  $a/b_1 = 0.6$ . At the low-frequency cutoff this error is at most 2 percent in the range  $0.5 \leq a/b_1 \leq 0.8$ . The error is larger in the high-frequency cutoff because here there is equal power in the fundamental and  $K = -1$  harmonics [7], [9]. Table I has been constructed for a certain corrugation geometry. If the corrugation were still denser, the errors would be smaller in all columns. Table I can be used to estimate the error in further calculations where the waveguide consists of a more complicated geometry or is partly filled with a dielectric material.

### B. A Tridepth Corrugated Waveguide

The geometry of a tridepth corrugated waveguide is shown in Fig. 1(b). This waveguide could be used in applications where ideal characteristics are required in three different frequency bands. As in the dual-depth case, we assume the slots and ridges to have constant width. The equivalent admittance  $y_0$  of the fundamental component is now

$$y_0 = \frac{p}{d} \frac{1}{S_0^2} \frac{y_1 y_2 y_3}{y_1 y_2 + y_2 y_3 + y_1 y_3} \quad (22)$$

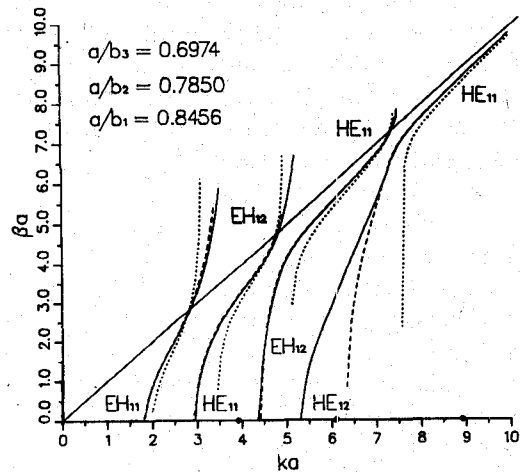


Fig. 4. Dispersion curve for an empty tridepth corrugated waveguide. The parameters are  $a/b_1 = 0.8457$ ,  $a/b_2 = 0.785$ ,  $a/b_3 = 0.6974$ ,  $t/d = 0.15$ , and  $d/a = 0.10$ . The balanced frequencies are marked by the spots. The solid line refers to the surface impedance method (eqs. (9) and (22)), the dashed line refers to the variational method with the cubic test function and the optimized parameters (eqs. (1), (4)–(7)). The dotted line refers to the analytical equation (8).

and when this is substituted in the eigenvalue equation (9), an approximative dispersion curve of the guide is obtained. The corrugation period equals  $p = 3t + 3d$ . The single admittance can be calculated from (18) by inserting given geometrical values. The dispersion relation of the tridepth guide with the combination  $a/b_1 = 0.6974$ ,  $a/b_2 = 0.785$ , and  $a/b_3 = 0.8456$  is considered. This corresponds to the frequency ratio 1:1.584:2.376 and to the frequencies 12.5 GHz, 19.8 GHz, and 29.7 GHz which are taken from satellite propagation experiments. The exact balance frequencies were calculated to be at  $ka = 3.9889$ ,  $6.0901$ , and  $8.9477$ . The other parameters were  $t/d = 0.15$  and  $d/a = 0.10$ . Assuming that there are three slots per wavelength at the highest frequency, i.e.,  $\lambda/(t+d) = 3$ , we have  $t = 0.4$  mm and  $d = 2.9$  mm. On the other hand, in order to obtain an acceptable cross-polarization level, this number should be at least 7 [1]. Then,  $t = 0.2$  mm and  $d = 1.25$  mm, values which it may still be possible to realize.

The eigenvalue equation of the guide is plotted in Fig. 4, where the solid curve stands for the eigenvalue equation

(9) and for (22). The dashed and the dotted lines indicate the variational results of the analytical equation (8) and of the functional with the cubic test function and optimized parameters. The admittance of the single slot is approximated by (21). The  $HE_{11}$  dispersion curve now has three different branches, because the short-circuit boundary condition, where the combination of the slots appears to act as a smooth-wall waveguide, occurs at two points where the denominator in (22) equals zero. These points,  $ka = 4.6072$  and  $7.2081$ , lie between the balanced frequencies, marked as spots in Fig. 4. The variational method works well again, except near the low frequency cutoff of the  $HE_{12}$  mode.

#### IV. DIELECTRICALLY LOADED CORRUGATED WAVEGUIDES

Here we apply the variational functional (1) for a corrugated waveguide which is partly filled with a dielectric material. The idea of this structure emerges from a tedious and costly fabrication of the corrugated waveguide. Normally one has to fabricate the guide by carefully lathing the metal pipe from the inside. If the corrugation is very dense, as is the case in, e.g., satellite communications and millimeter-wave remote sensing applications, the widths of the slots and the ridges are of the order of 1 mm or even less. Then it is often very difficult to move the cutter of the lathe from one slot to the other so that the ridge between the slots is not bent. In addition, metal chips may remain in the slot, which then cause short circuits. As a result, the corrugation geometry is not the one required, and the performance of the guide falls off. These difficulties can be avoided by using a different fabrication method: a dielectric rod is put in the lathe, grooves are made on the outside, and the outer surface is metallized. Finally, a hole is drilled on the axis, and a dielectrically loaded corrugated waveguide is finished. This idea was suggested by Prof. Tiuri, and such a waveguide possessing a single-depth corrugation was analyzed by the present variational method by Lindell *et al.* [8]. They showed that in the limit case where the dielectric insert covers only the corrugation, dielectric losses are less than 10 percent from conductor power losses at 10 GHz. The corrugation parameters were  $d/(d-a) < 0.5$  and  $(b-a)/\lambda < 0.1$ .

Dispersion relations for the dielectrically loaded dual-depth and tridepth guides are given in Figs. 5, 6, and 7. The curves have been calculated by applying the functional (1) with the cubic test functions (4) and (5) and the admittance formulas (11) and (22). The equivalent admittance for a single slot has been approximated by (21). The magnetic field coefficient  $A$  in (5) can again be optimized analytically, although the result is much more complicated than that for the empty guide (eq. (6)). The parameter  $\alpha$  must now be determined by a numerical routine.

The results for the dual-depth guide are shown as a function of  $\beta/k$  for different  $ka$  values and for three values of the thickness of the loading layer:  $c/a = 0.95$ , 0.90, and 0.80. Also,  $t/d = 0.15$  and  $d/a = 0.10$ . The dielectric insert is Teflon with  $\epsilon_r = 2.08$ . At higher frequen-

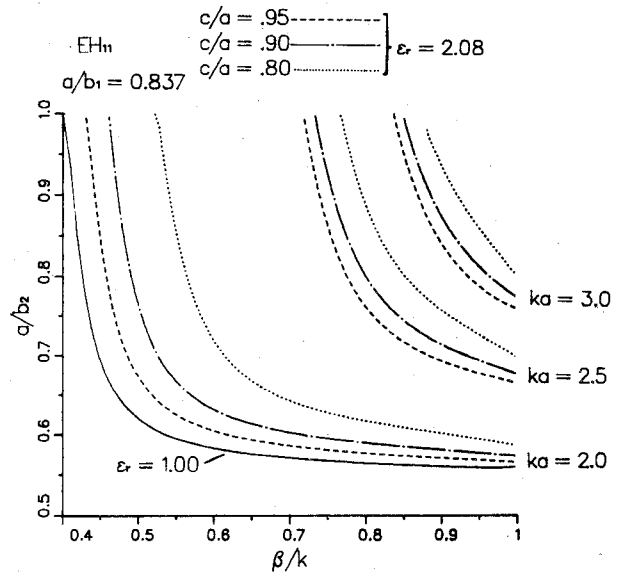


Fig. 5. Uniform dispersion curves of the  $EH_{11}$  mode in a dielectrically loaded dual-depth corrugated guide. The curves have been evaluated by the variational functional (1) with the cubic test functions (4)–(7) for three different dielectric layer thicknesses  $c/a$ . The dielectric insert is Teflon with  $\epsilon_r = 2.08$ .  $t/d = 0.15$  and  $d/a = 0.10$ .

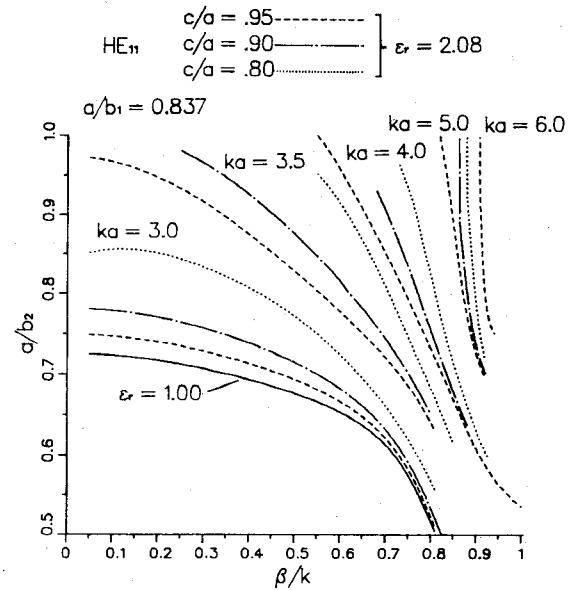


Fig. 6. Same as in Fig. 5 for the  $HE_{11}$  mode.

cies in Fig. 6 the curve becomes more and more vertical, which indicates that here the dispersion curve has a weaker dependence on the dielectric insert and on the corrugation geometry. This means also that Figs. 2 and 3 serve for the dielectrically loaded guide, at least in the region of large  $ka$  values. In Fig. 7 the dispersion curves of the tridepth guide with the dielectric load are plotted. For comparison, the dispersion curves of the empty guide are also shown. The thickness parameter  $c/a$  is now 0.95 and the dielectric load is again Teflon. The corrugation parameters are those of the empty guide. The dispersion curves follow very closely the empty guide curves in the regions of interest.

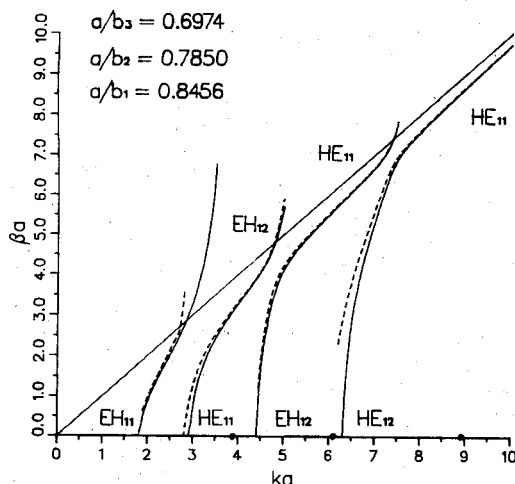


Fig. 7. Dispersion curve for an empty (solid line) and for a dielectrically loaded (dashed line) tridepth corrugated waveguide. The geometrical parameters are  $a/b_1 = 0.8456$ ,  $a/b_2 = 0.785$ ,  $a/b_3 = 0.6974$ ,  $t/d = 0.15$ ,  $d/a = 0.10$ , and  $c/a = 0.95$ . The dielectric insert is Teflon with  $\epsilon_r = 2.08$ . The curves have been calculated by the variational functional (1) with the cubic test functions (4) and (5).

## V. CONCLUSION

The nonstandard variational method was applied to the dielectrically loaded multidepth corrugated waveguide. The method was first tested for the empty dual-depth guide, where by using simple linear and cubic test functions with few optimizable parameters, accurate dispersion curves were obtained. The linear test function led to an analytical dispersion formula which is very easy to use compared with all other methods available in the literature. The cubic test function was seen to give more accurate results and was attractive because all parameters in the test function could be optimized analytically. The variational results were compared with the results obtained by the surface impedance and by space-harmonic methods. A new corrugated waveguide whose corrugation period consists of three different slot depths was introduced and its

dispersion characteristics were calculated. Finally, the method was used to analyze a dielectrically loaded corrugated guide, a component which may be realistic because of its easier fabrication technique.

## REFERENCES

- [1] A. D. Olver, K. K. Yang, and P. J. Clarricoats, "Propagation and radiation behaviour of dual-depth corrugated horns," *Proc. Inst. Elec. Eng.*, vol. 131, pt. H, pp. 179-185, June 1984.
- [2] S. Ghosh, "A corrugated waveguide feed for discrete multiband applications having dual depth corrugation," in *Proc. IEEE/AP-S Int. Symp.* (Quebec), June 1980, pp. 217-220.
- [3] N. Sridhar and G. P. Srivastava, "Theoretical analysis of hybrid modes in a dual-depth corrugated waveguide feed," *Electron. Lett.*, vol. 18, pp. 793-794, Sept. 1982.
- [4] Z. Rirong and W. Hanli, "Analysis of a new corrugated guide feed horn having dual-depth corrugations," *Radio Sci.*, vol. 17, pp. 747-751, July-August 1982.
- [5] Y. Kezhong, W. Hanli, and Z. Rirong, "Propagation and radiation behaviour of corrugated circular waveguide having dual depth combination," *Scientia Sinica (A)*, vol. XXVI, pp. 990-1003, Sept. 1983.
- [6] A. D. Olver, P. Yang Kezhong, and P. J. B. Clarricoats, "Dual-depth corrugated horn design," in *Proc. 13th European Microwave Conf.* (Nürnberg, West Germany), Sept. 1983, pp. 879-844.
- [7] Y. Kezhong, Z. Rirong, and W. Hanli, "Corrugated circular waveguide with dual-depth corrugations," *Scientia Sinica (A)*, vol. XXVIII, pp. 1098-1114, Oct. 1985.
- [8] I. V. Lindell and A. H. Sihvola, "Dielectrically loaded corrugated waveguide: Variational analysis of a nonstandard eigenproblem," *IEEE Trans. Microwave Theory Tech.*, vol. MTT-31, pp. 520-526, 1983.
- [9] P. J. B. Clarricoats and A. D. Olver, *Corrugated Horns for Microwave Antennas*. London: Peter Peregrinus, 1984.

✖

Markku I. Oksanen was born in Jyväskylä, Finland, on December 1, 1958. He received the degrees of Diploma Engineer and Licentiate of Technology in electrical engineering in 1983 and 1987, respectively. From 1983 to 1984, he was a Research Engineer at the Radio Laboratory, Helsinki University of Technology, and from 1984 to 1986 a Research Engineer at the Technical Research Center of Finland. Since 1986 he has been at the Electromagnetics Laboratory, Helsinki University of Technology. He is currently pursuing a course of study for the doctor's degree in electrical engineering. His interests are in waveguide theory and antennas.

